The Seismic Record
A journal of the Seismological Society of America

Variability in the Natural Frequencies of a Nine-Story Concrete Building from Seconds to Decades

Ethan F. Williams*[1], Thomas H. Heaton[1,2], Zhongwen Zhan[1], and Valere R. Lambert[3]

Abstract

Since 2001, the Southern California Seismic Network has archived continuous waveform data from strong-motion station CI.MIK in Caltech Hall (formerly Millikan Library)—a nine-story reinforced concrete building. Simple spectral analysis of this 20 yr record reveals that the building's fundamental frequencies have increased gradually by 5.1% (east–west) and 2.3% (north–south), with larger long-term variability up to 9.7% (east–west) and 4.4% (north–south). This finding is unexpected, as previous analysis of forced vibration tests and strong-motion records has shown that between 1968 and 2003 the fundamental frequencies decreased by 22% (east–west) and 12% (north–south), largely attributed to minor structural damage and soil–structure system changes from major earthquakes. Today, the building's apparent structural stiffness is comparable to what it was in 1986, before the Whittier Narrows earthquake. Using data from earthquakes and forced vibrations, we also document the building's nonlinear dynamic elasticity, which is characterized by a rapid softening (decrease in apparent frequencies) at the onset of strong motion, followed by a slower, log–linear recovery trend over the scale of minutes. This nonlinear behavior does not appear to have changed with time.

Cite this article as Williams, E. F., T. H. Heaton, Z. Zhan, and V. R. Lambert (2022). Variability in the Natural Frequencies of a Nine-Story Concrete Building from Seconds to Decades, *The Seismic Record*. **2**(**4**), 237–247, doi: 10.1785/0320220032.

Supplemental Material

Introduction

Reliable estimation of the natural frequencies of a building is essential for earthquake and structural engineering practice, from design-stage fragility analysis to postearthquake damage assessment. Current engineering approaches rely on the assumptions that the natural frequencies, serving as a proxy for stiffness, are time invariant and follow linear elasticity up to the yield point. For example, widely employed intensity measures like spectral acceleration filter design ground motions through a linear, time-invariant harmonic oscillator (e.g., Baker *et al.*, 2021). Even nonlinear methods, such as nonlinear response history analysis, typically assume linear elasticity and only consider large strain and material inelasticity or elastoplasticity (e.g., Haselton *et al.*, 2017; Zimmerman *et al.*, 2017). However, the exponential proliferation of digital seismographs over the past several decades has shown that these assumptions poorly describe the behavior of many classes of structures. Numerous examples have been reported of nondamaging earthquakes causing temporary softening of the soil–structure system that recovers rapidly after shaking (Udwadia and Trifunac, 1974; Trifunac *et al.*, 2001; Astorga *et al.*, 2018), as well as small permanent changes (Clinton *et al.*, 2006). Nonearthquake loading by wind or anthropogenic vibrations has been observed to have a similar effect (Kohler *et al.*, 2005; Clinton *et al.*, 2006; Gueguen *et al.*, 2016). These effects have been variously interpreted as the result of small-strain nonlinear elasticity of construction materials, reactivation of fractures in the previously damaged structural elements, nonlinear elasticity or elastoplasticity of foundation soils, or some combination thereof. Passive environmental

1. Seismological Laboratory, California Institute of Technology, Pasadena, California, U.S.A., https://orcid.org/0000-0002-6471-4497 (EFW); https://orcid.org/0000-0003-3363-2197 (THH); https://orcid.org/0000-0002-5586-2607 (ZZ); 2. Department of Mechanical and Civil Engineering, California Institute of Technology, Pasadena, California, U.S.A.; 3. Department of Earth and Planetary Sciences, University of California, Santa Cruz, Santa Cruz, California, U.S.A., https://orcid.org/0000-0002-6174-9651 (VRL)

*Corresponding author: efwillia@caltech.edu

changes also have a marked impact on apparent structural stiffness, including positive correlations with temperature and rainfall (Clinton *et al.*, 2006; Todorovska and Al Rjoub, 2006).

To date, studies of anomalous changes in the natural frequencies of civil structures have largely focused on relatively short-time scales due to the paucity of long, continuous waveform records. Consequently, the long-term stability of these frequencies over the lifetime of a structure is not generally understood. In this article, we quantify the variability and long-term changes in the first six natural frequencies of Caltech Hall, a nine-story reinforced concrete building, over a span of 20 yr from 2001 to 2021. Formerly known as the Robert A. Millikan Memorial Library (or Millikan Library), Caltech Hall has been the subject of extensive study since its construction in 1967. Initially subject to minor damage in the 1971 San Fernando earthquake and repeatedly shaken by subsequent southern California earthquakes, the fundamental frequencies of Caltech Hall in the east–west and north–south directions decreased by 22% and 12%, respectively, from 1968 to 2002 (Clinton *et al.*, 2006). What changes occurred between these major events are only illuminated by a temporally scattered record of forced and ambient vibration tests. In 2001, the Southern California Seismic Network (SCSN) installed a triaxial accelerometer (station CI.MIK) on the ninth floor of the building and began archiving continuous waveform data. Clinton *et al.* (2006) examined the initial 1.5 yr of data from CI.MIK, documenting the response of the building to environmental forcing on the scale of hours to weeks and three small earthquakes. The 20 yr continuous record up to the present provides the opportunity not only to examine frequency variations over much longer time scales, but also construct a continuous spectrum of nonlinear elasticity with almost 700 regional and local earthquakes.

Background and Data

Caltech Hall is a nine-story reinforced concrete building on the campus of the California Institute of Technology (Caltech) in Pasadena, California (Fig. S1, available in the supplemental material to this article). The 44 m superstructure consists of a reinforced concrete moment frame, two north–south-oriented reinforced concrete shear walls on the east and west faces of the building, and a reinforced concrete central core. Below a 4 m basement level, the structure is supported by a concrete pad foundation that runs east–west across the center of the building joining the shear walls. For a detailed description of the structure, see Kuriowa (1967), Favela (2004), Clinton *et al.* (2006), and references therein. As a result of this construction, the responses of the building in the east–west and north–south directions differ dramatically. The apparent system frequencies of Caltech Hall—that is, the frequencies measured from peaks in the ambient vibration spectrum of a station in the building—include the coupled effects of the fixed-base stiffness of the superstructure, and the shearing and rocking stiffness of the soil–foundation system (Luco *et al.*, 1987). In particular, as a result of the shear-wall geometry, the north–south deformations are dominated by rigid-body rocking, whereas east–west deformations more closely approximate fixed-base shearing (Luco *et al.*, 1988). Whether earthquake-related changes in the natural frequencies of Caltech Hall should be attributed to changes in structural stiffness (Luco *et al.*, 1987) or soil–structure interaction (Todorovska, 2009a) has been a subject of considerable historical debate.

We utilize recordings from strong-motion station CI.MIK, located on the ninth floor of Caltech Hall, over a 20 yr period from May 2001 to May 2021. Since 2001, CI.MIK has been instrumented with a Kinemetrics EpiSensor ES-T triaxial accelerometer, and continuous waveform and event data have been archived by the Southern California Earthquake Data Center (SCEDC). There is a gap in continuous waveform data from the SCEDC archive in 2008–2009, but event data from this period are available.

Long-Term Changes

To track the time-dependent variation of the natural frequencies of Caltech Hall, we apply a simple frequency–time analysis to the continuous waveform data. For ambient vibrations, we use the Fast Fourier Transform to calculate the power spectral density (PSD) for each hour of data, compute the weekly median PSD, and pick the maximum value in a 0.2 Hz band around each modal frequency. We refer to Bradford *et al.* (2004) for modal identification (see Fig. S2). Because the frequencies generally vary smoothly with time on the scale of weeks to months and do not overlap, automatic tracking of the modal peak is therefore possible, and computing a weekly median effectively removes strong diurnal trends from temperature and building use. Weekly median spectrograms are plotted in Figure 1 for the first six natural frequencies of Caltech Hall, exhibiting a complex superposition of seasonal and interannual trends. A complete summary of changes and variability for each frequency is given in Table S1.

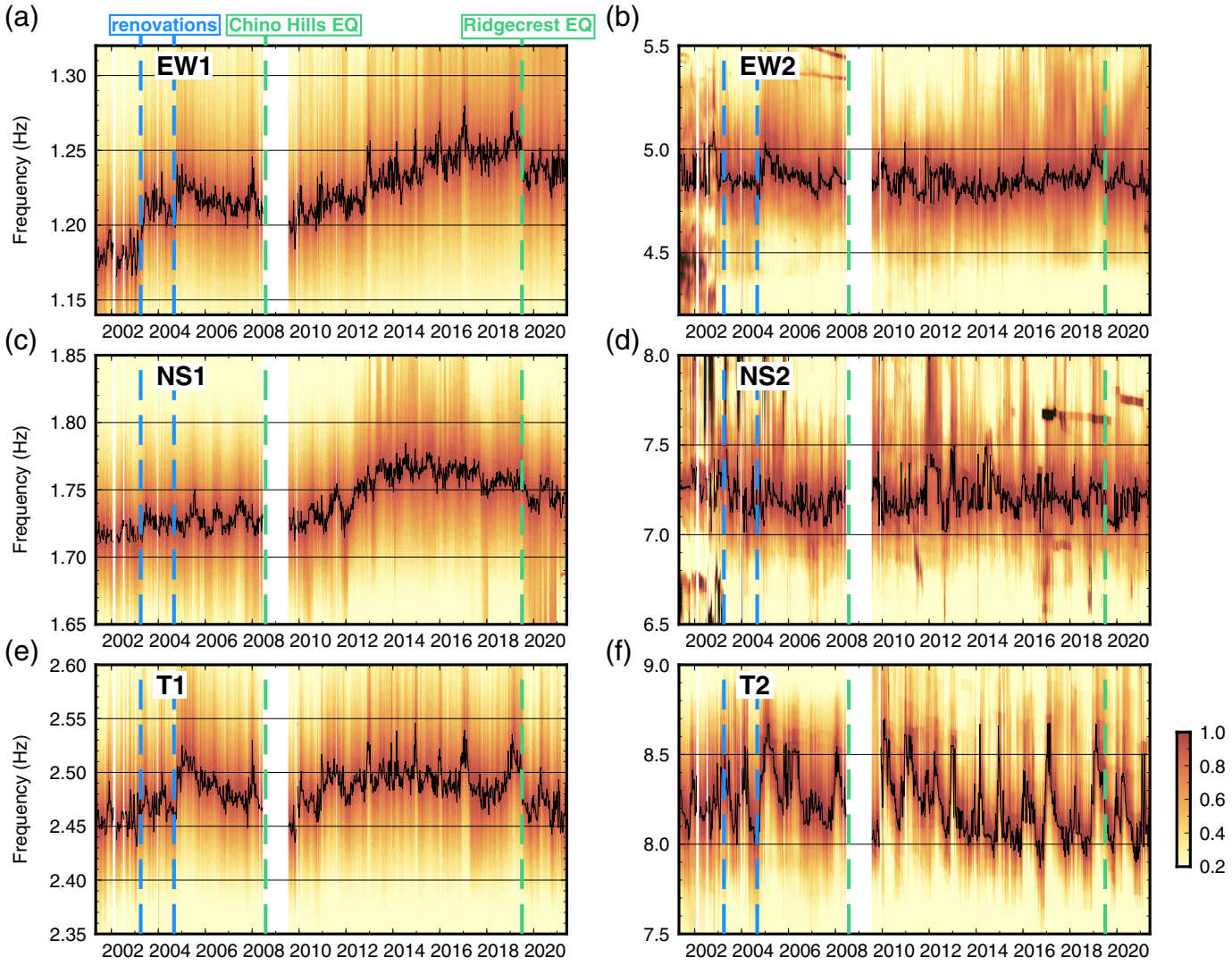

Interannual trends

Comparing the median frequencies from the months of May 2001 and May 2021, the fundamental frequency in the east–west direction (hereafter, EW1) increased by 5.1%, from 1.18 to 1.24 Hz (Fig. 1a), which is equivalent to a 10.4% increase in the apparent stiffness of the combined soil–structure system ($f \propto \sqrt{k/m}$, in which k is stiffness and m is mass). The fundamental frequency in the north–south direction (NS1) increased by 2.3% over this time period, from 1.71 to 1.75 Hz (Fig. 1c), or a 4.7% increase in apparent stiffness. The 20 yr net change in EW1 and NS1 can be further divided into a combination of discrete events and gradual trends. The first major increase in the apparent stiffness of Caltech Hall occurred during two stages of nonstructural renovations converting library floors into office space during spring 2003 and fall 2004. The first of these projects had the greatest impact on the fundamental frequencies EW1 and NS1, whereas the second had a larger impact on the torsional fundamental

Figure 1. Long-term changes in the first six frequencies of Caltech Hall from ambient vibrations. (a,b) Spectrograms of CI.MIK.BLE and CI.MIK.BNE from May 2001 to May 2021, enlarged to show the (a) first and (b) second natural frequencies of the east–west system. The color scale has been normalized in each frequency bin from decibels relative to 1 count. A median filter was applied to panel (b) along the frequency axis to reduce artifacts from motors in the building with similar vibrational frequencies (see spikes in Fig. S2). (c,d) Same as panels (a,b) but for CI.MIK.BLN and CI.MIK.BNN showing the first two frequencies of the north–south system. (e,f) Same as panels (a,b), but for the torsional frequencies measured on the east–west seismometer component. Black lines indicate the weekly median frequency.

frequency (T1) and the first east–west overtone (EW2; Fig. 1). Following each sharp increase in 2003–2004, all affected frequencies decreased gradually at varying rates until around 2008. As discussed by Clinton *et al.* (2006), who also examined the first of these renovation projects, the fractional magnitude of the increase in apparent structural stiffness is surprisingly large: EW1 increased ∼3% over three months in 2003 and ∼2% over one month in 2004. Further, it is unclear why such work could have initiated a softening trend, as construction materials like adhesives tend to stiffen with time after application (e.g., Moussa *et al.*, 2013).

From late 2009 (following a data gap), the fundamental frequencies EW1 and NS1 began a period of gradual increase, indicating apparent healing of the soil–structure system. EW1 increased at a rate of ∼1%/yr until around 2017, when the trend slowed. At its maximum in January 2017, EW1 was up 8.5% from May 2001 or +17.7% apparent stiffness. Although NS1 also increased during this time period, the timing of changes in the two frequencies are not clearly correlated. NS1 increased rapidly from 2012 to 2014 and peaked in mid-2014 at a 4.1% increase relative to May 2001. Starting in 2016, NS1 began to decrease again, whereas EW1 remained approximately constant. We are not aware of any environmental trends or construction work that correlate with the observed interannual trends in apparent stiffness.

Over this period, Caltech Hall was subject to only two moderate regional earthquakes. The 2008 **M** 5.4 Chino Hills earthquake coincides with the change in interannual behavior of both EW1 and NS1, though it is unclear why strong motion would induce a decade-long healing trend when there was no apparent permanent coseismic decrease in stiffness. The **M** 6.4 and 7.1 Ridgecrest earthquakes in 2019, however, did result in a 2.5% permanent decrease in EW1 and 1.6% decrease in T1, despite peak east–west accelerations at CI.MIK of only 0.77 and 0.75 m/s^2 for the two events. This permanent softening is comparable in magnitude to the inferred historical changes in EW1 from the 1988 M 6.1 Whittier Narrows and 1994 M 6.7 Northridge earthquakes, when the peak east–west accelerations at the upper floors of Caltech Hall were observed to be much higher at 2.62 and 1.43 m/s^2, respectively (Clinton *et al.*, 2006). Despite this recent softening, the apparent fundamental frequencies of the combined soil–structure system from ambient vibrations are comparable today to their values before the Whittier Narrows, Sierra Madre, and Northridge earthquakes, indicating a significant net increase in stiffness.

Seasonal variability

The natural frequencies of Caltech Hall also exhibit seasonal variability (Fig. 2). Clinton *et al.* (2006) previously observed a rapid increase in the fundamental frequencies over the scale of 1–2 days during periods of rain, followed by recovery over the scale of a week with NS1 least affected. The 20 yr record of weekly median measurements of EW1 and T1 shows a sharp increase of up to ∼3% in winter months coincident with periods of rainfall consistent with the short-term observations (Fig. 2a). In years with longer separation between storms, such as 2013 and 2017, the seasonal effect of rainfall is negligible; however, in years with a concentrated period of rainfall over 1–2 months, such as 2012, the cumulative increase in stiffness is greater. Poroelastic effects in saturated soil increase the horizontal stiffness of an embedded foundation (Todorovska and Al Rjoub, 2006), which suggests that the time scale of the precipitation-induced increases in EW1 and T1 is related to the drainage time scale of shallow soil. However, the first torsional overtone (T2) surprisingly exhibits a much larger increase, up to ∼9%, during periods of heavy rainfall, and the change in T2 decays slowly over the scale of a year, unlike EW1 and T1 (Fig. 2c). Ghahari *et al.* (2015) found that the flexible-base mode shape for T2 includes significant vertical displacement, which suggests a higher dependence on the vertical stiffness of the soil–foundation system relative to EW1 and T1. The variability of T2 correlates well with modeled soil moisture (Rodell *et al.*, 2004), which serves as a proxy for the depth to fully saturated soil. Changes in EW1 and T1 after rainfall may thereby diminish quickly as the <4 m shallow soil buttressing the foundation drains, decreasing the horizontal foundation stiffness; whereas changes in T2 may diminish slowly as the water table draws down and the integrated vertical stiffness of subfoundation soil decreases.

On a seasonal scale, NS1 is largely unaffected by precipitation but shows the greatest sensitivity to temperature with an approximate increase of 1% per 10° C (Fig. 2b). This is inconsistent with the short-term observations of Clinton *et al.* (2006), who showed that diurnal variations in temperature have a similar influence on all fundamental frequencies. The shear walls on the east and west faces of Caltech Hall are 30.5 cm thick, whereas the thermal skin depth for diurnal forcing is around 5–10 cm ($\sqrt{2\kappa/\omega}$, for κ ∼0.1–0.5 mm^2/s), suggesting that seasonal temperature changes will have a greater thermal expansion effect on the shear walls than diurnal variations.

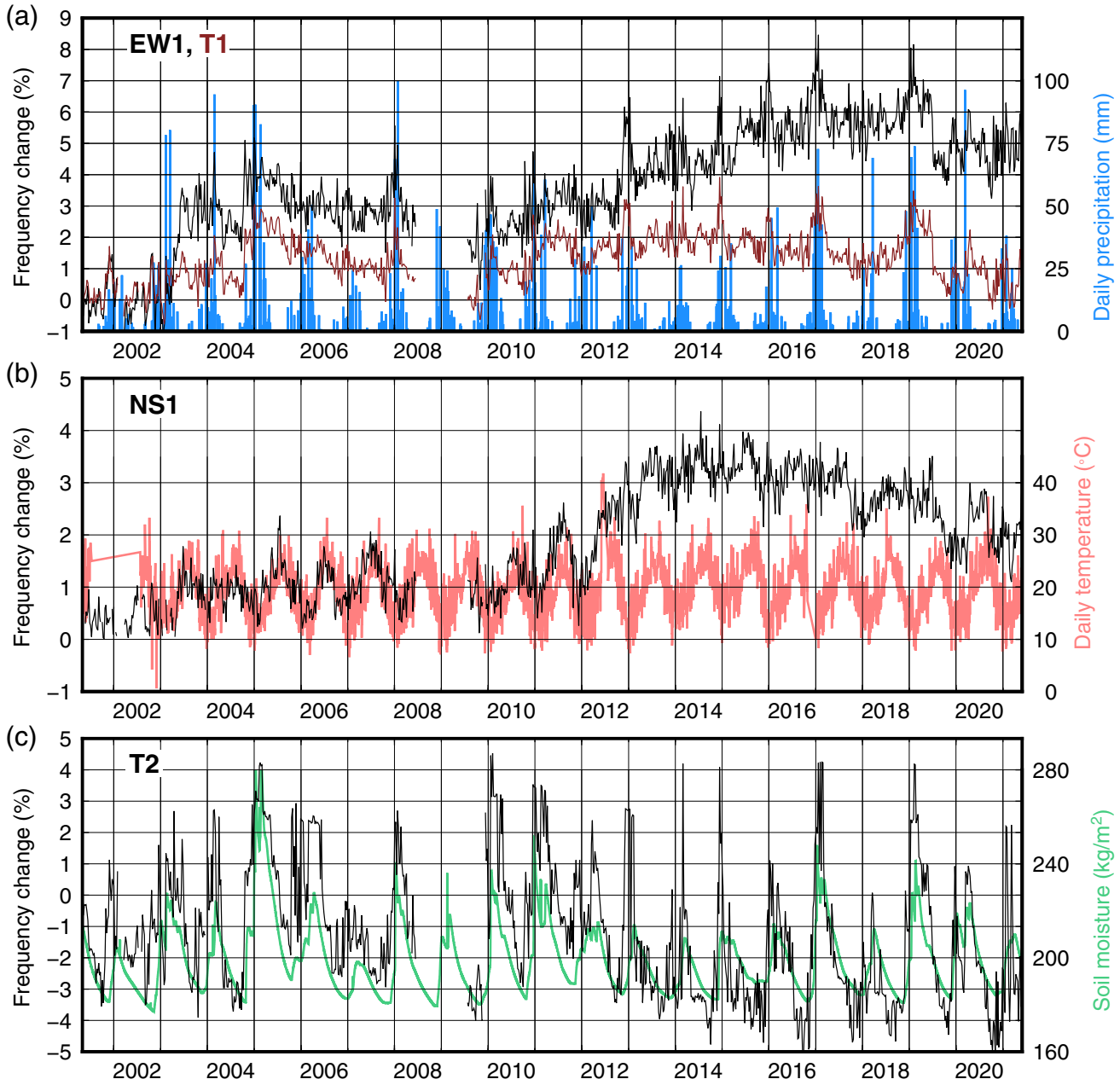

Short-Term Changes

To document the response of Caltech Hall to earthquake loading, we downloaded 684 regional earthquakes, representing all SCEDC cataloged events with **M** > 4 and peak acceleration at CI.MIK >0.001 m/s^2 between May 2001 and May 2021. For each event we define the apparent event frequency in the east–west and north–south directions as the peak in the PSD of a 60 s record beginning at the *P*-wave arrival. For a subset of 54 events with peak acceleration >0.01 m/s^2 and excluding closely spaced aftershocks, we compute the spectrogram of a

Figure 2. Seasonal and interannual changes in the natural frequencies of Caltech Hall from ambient vibrations compared with environmental data. (a) Fractional changes in the fundamental east–west and torsional frequencies relative to May 2001 compared with daily precipitation from the Climate Hazards Group InfraRed Precipitation with Station data (CHIRPS) rainfall database (Funk *et al.*, 2014). (b) The fundamental north–south frequency compared with daily mean temperature measurements at nearby Santa Fe Dam from the Global Historical Climatology Network daily (GHCNd) database (Menne *et al.*, 2012). (c) The second torsional frequency compared with soil moisture at 100–200 cm depth extracted from the Global Land Data Assimilation System (GLDAS-2.1) model (Rodell *et al.*, 2004).

five-minute record and pick the apparent frequencies in each time window to track the postearthquake recovery of the building. The apparent event frequency is generally proportional to and slightly higher than the minimum frequency derived from time–frequency analysis because the minimum frequency is always coincident with the peak acceleration, but is more stable for small events. We also supplement earthquake data with new and historical forced vibration tests (Table S2).

Nonlinear response

The apparent event frequency for all 684 earthquakes is plotted in Figure 3 against time and peak acceleration. For both EW1 and NS1, earthquakes clearly follow the same seasonal and interannual trends as measured from ambient vibrations, though the variability is higher due to the combination of a nonlinear reduction in frequency with strong motion and the rapid wander of the building's frequencies on subweekly time scales not captured by the ambient vibration curve (Fig. 3a,c). A decrease in the apparent frequencies of Caltech Hall with increased shaking intensity was first noted by Kuriowa (1967) during forced vibration tests. Clinton *et al.* (2006) compiled available earthquake records through 2004, mostly exceeding 0.1 m/s^2 peak acceleration, and noted a power law scaling between the apparent event frequency and peak acceleration. Extending this analysis with all events 2001–2021, we observe that the nonlinear relationship between apparent frequency and acceleration persists continuously down to at least 0.001 m/s^2, close to the intensity of ambient vibrations (Fig. 3b,d). Importantly, there is no linear elastic regime for any level of excitation. We also repeated the experiment of Kuriowa (1967) in November 2019 and conducted forced vibration tests to measure EW1 at six different levels of forcing. These results are plotted as black crosses in Figure 3b, and follow the same relationship between frequency and acceleration as exhibited by earthquakes, suggesting that peak acceleration is an adequate single intensity measure and the influence of other factors like shaking duration is comparatively small.

A single power law relationship, however, poorly describes the complete spectrum of nonlinear behavior from 0.001 to >1 m/s^2. Rather, we identify a weakly nonlinear regime and a strongly nonlinear regime separated by a transition acceleration around 0.02–0.04 m/s^2, which is higher for NS1 than EW1. A factor of 10 increase in acceleration for EW1 results in an ∼3% reduction in apparent frequency in the weakly nonlinear regime and an ∼9% reduction in the strongly nonlinear regime (1.5% and 6%, respectively, for NS1). In addition to the difference in scaling, these two regimes exhibit distinct time-dependent behavior. Separating all events into two bins from 2001 to 2011 and 2011 to 2021, for both EW1 and NS1 the long-term increasing trend in apparent stiffness manifests as a uniform upward shift in the event frequencies across the weakly nonlinear regime, with no difference in slope (Fig. 3e,f). Conversely, there is no statistically significant change in either the slope or the mean event frequency across the strongly nonlinear regime for either EW1 or NS1, though the relatively small number of strong events contributes to large uncertainty bounds at high accelerations. Todorovska (2009a) found that the rocking stiffness in the north–south direction of Caltech Hall decreases dramatically during strong motion, whereas the reduction in the stiffness of the superstructure is less. If the reduction in the rocking stiffness can be attributed to nonlinear elastic or elastoplastic soil–structure interaction above a small-strain threshold, then the weakly and strongly nonlinear regimes may be distinguished by the relative contributions of the superstructure and soil–foundation system to the apparent dynamic softening of the combined system. Such effects cannot be separated, however, using a single station analysis.

Log–linear recovery

Although a small permanent reduction in the natural frequencies of Caltech Hall has been observed for nondamaging historical earthquakes, the frequencies recover rapidly to their pre-event levels for the majority of events (Clinton *et al.*, 2006). Such rapid dynamic softening (often termed anomalous nonlinear fast dynamics or ANFD) followed by slow recovery (often termed slow dynamics) has been widely documented in laboratory rock mechanics (tenCate *et al.*, 2000; Johnson and Sutin, 2005) and recently reported for several structures (Kohler *et al.*, 2005; Gueguen *et al.*, 2016; Astorga *et al.*, 2018; Astorga and Gueguen, 2020). Example spectrograms with a resolution of 12.8 s are plotted in Figure 4 for two earthquakes, showing that the apparent system frequencies of Caltech Hall drop suddenly at the onset of strong motion and then recover slowly following an approximately log–linear curve over the scale of minutes. For these two events—the 2007 **M** 4.7 Trabuco Canyon (Fig. 4a–d) and 2008 **M** 5.4 Chino Hills (Fig. 4e–h) earthquakes—the peak acceleration at CI.MIK differs by a factor of 10, but the recovery curves follow a similar trend. The relative recovery of the apparent frequency in each time

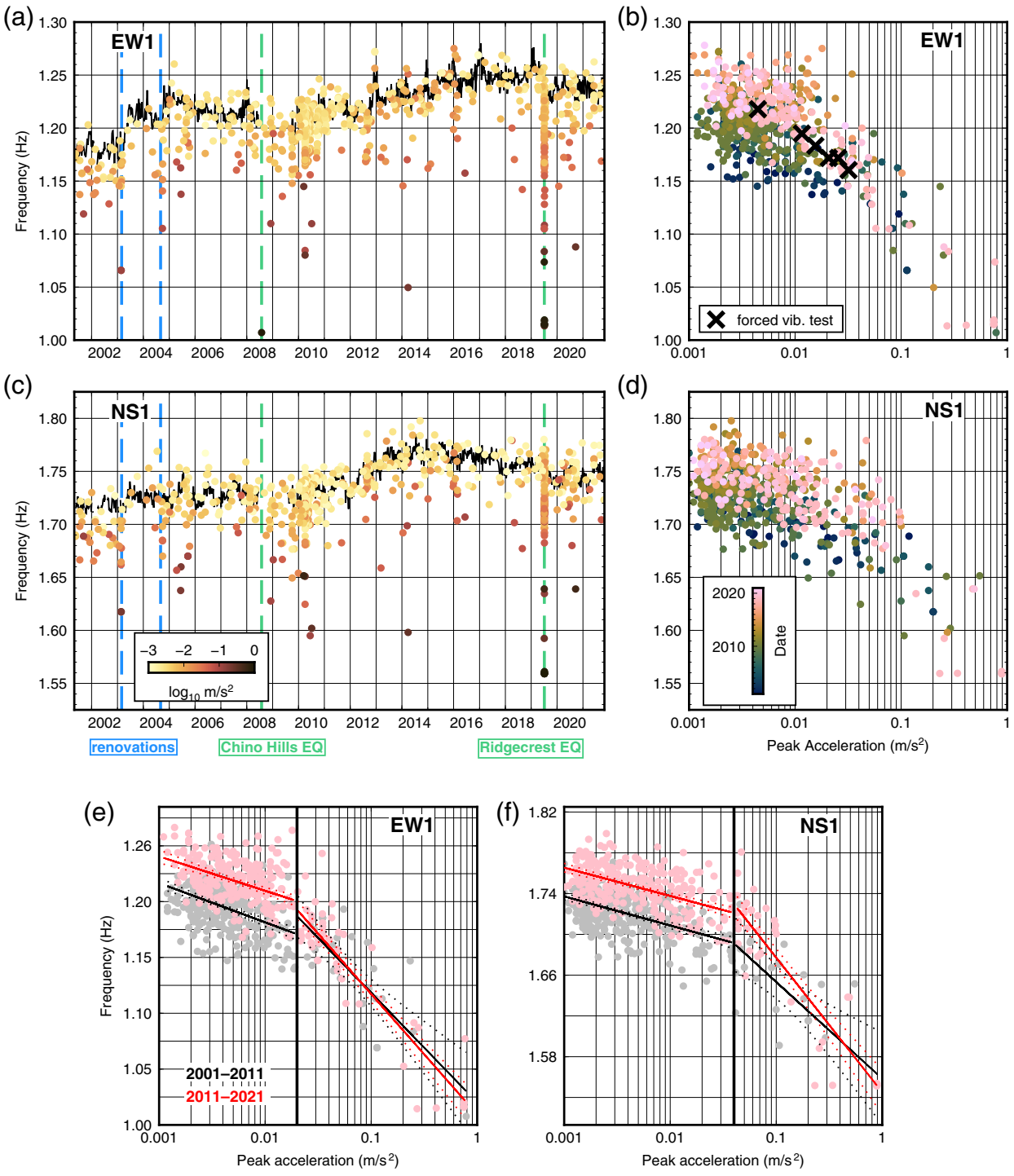

Figure 3. Response of Caltech Hall to 684 local and regional earthquakes >**M** 4 between 2001 and 2021. (a) Apparent east–west fundamental frequency for each earthquake plotted against the ambient vibration curve (black line) and colored by peak acceleration at CI.MIK. (b) Same data as in panel (a), but plotted against peak acceleration and colored by date, compared with forced vibration tests (black crosses). (c,d) Same as panels (a,b), but for the apparent fundamental frequency in the north–south direction. (e,f) Same as panels (b,d) on a log–log scale with earthquakes divided between the periods 2001–2011 (black) and 2011–2021 (red). The trends in nonlinear response are illustrated with a linear regression (solid lines), and 95% confidence interval (dashed lines) above and below a transition frequency. Note that a few of the largest events are truncated from these plots.

window, $(f - f_{min})/(f_0 - f_{min})$, is reasonably well described by a log–linear function of time (Fig. 4i,j) and is 85%–95% recovered after five minutes for both the earthquakes. We extended this analysis to all 54 events with peak acceleration >0.01 m/s^2, and the mean and standard deviation of regressed recovery rates are expressed as gray shading in Figure 4i,j. Even though the scatter among individual events is large, likely due to order of magnitude variations in shaking duration, the average trend highlights that ~20% recovery typically occurs rapidly after the peak acceleration, and ~80% recovery occurs within 5 min. There is no significant difference in recovery rate for either EW1 or NS1 and no significant change in recovery rate over the period of study.

Discussion and Conclusions

Since 2001, the natural frequencies of Caltech Hall have increased by 5.1% (EW1) and 2.3% (NS1). Although a fraction of the 20 yr change can be attributed to the installation of nonstructural office partitions in 2003–2004, the majority of the increase in apparent structural stiffness occurred gradually between 2009 and 2017, and is not clearly correlated with any environmental trends or construction work. In the only other comparable longitudinal study of a building to date, Astorga *et al.* (2018) showed that the natural frequencies of a steel and reinforced concrete building in Japan gradually decreased over a 12 yr period preceding the 2011 Tohoku–Oki earthquake. Such long-term softening is the expected lifetime behavior of reinforced concrete structures, as many well-documented mechanisms can contribute to degradation, such as fracture formation, thermal stressing, carbonation, and corrosion of rebar (Lees, 1992). The anomalous long-term stiffening of Caltech Hall is more difficult to explain. Minor cracking of the concrete slabs and shear walls at the ground floor level of the building were observed following the 1971 San Fernando earthquake, potentially associated with a reduction in foundation stiffness (Foutch and Jennings, 1978). One possible explanation is that migration of groundwater through cracks in the foundation could deposit calcite and heal the foundation concrete over long-time scales (e.g., Edvardsen, 1999; Roig-Flores and Serna, 2020). Alternatively, the cumulative effect of small and large building vibrations could act to compact the soil beneath the foundation and increase the stiffness. Incorporation of multistation records to decompose the superstructure and soil–foundation contributions to the apparent stiffness over time would be necessary to further probe the cause of the Caltech Hall's increasing stiffness. A second permanent SCSN accelerometer was installed at the basement level in 2008 (CI.MIKB), and Community Seismic Network accelerometers were installed on all floors in 2015, which may be utilized for seismic interferometry (e.g., Todorovska, 2009b) or to study temporal changes in the building's mode shapes.

Over 20 yr, the natural frequencies of Caltech Hall also exhibited an overall variability of 9.7% (EW1) and 4.4% (NS1). This variability should be considered the minimum estimate, as the weekly median frequency analysis discounts short-term effects of diurnal temperature changes, wind, and rainfall, which can be as large as 3% (Clinton *et al.*, 2006) and does not include the effect of amplitude-dependent nonlinear elasticity. Such large variability poses a significant challenge for structural health monitoring and postearthquake damage assessment. The observed variability exceeds the building's inferred permanent decrease in frequencies from the 1987 Whittier Narrows, 1991 Sierra Madre, and 1994 Northridge earthquakes (Fig. 5). Further, if the long-term healing of Caltech Hall has been a persistent trend throughout the building's 55 yr lifetime, then inferences from a scattered record of ambient and forced vibration tests may significantly underestimate the permanent changes from historical earthquakes (Fig. 5). Establishing a reliable baseline for structural health monitoring thereby requires continuous recording to correct for environmental trends and long-term changes that are aliased by sporadic monitoring. Even full-scale forced vibration tests may fail to identify moderate damage or falsely identify damage if conducted in isolation without considering the passive variations of a building's natural frequencies, as evidenced by the comparable variability of forced and ambient vibration tests over the last 30 yr (Fig. 5). The significant dynamic softening of Caltech Hall during strong motion for some nondamaging events such as the 2008 Chino Hills earthquake (Figs. 4 and 5) is comparable in magnitude to the temporary softening experienced during the 1971 San Fernando earthquake, which did cause minor damage, and in other buildings experiencing more significant damage (e.g., Trifunac *et al.*, 2001), suggesting that triggered strong-motion records may be insufficient to identify damage without a detailed model of a building's nonlinear elastic response. Triggered records are also typically too short to capture enough of the time-dependent recovery process to make an asymptotic inference of the final postevent frequencies (Udwadia and Trifunac, 1974; Fig. 4). We conclude that continuous recording should be a requirement for urban strong-motion networks, and that linear,

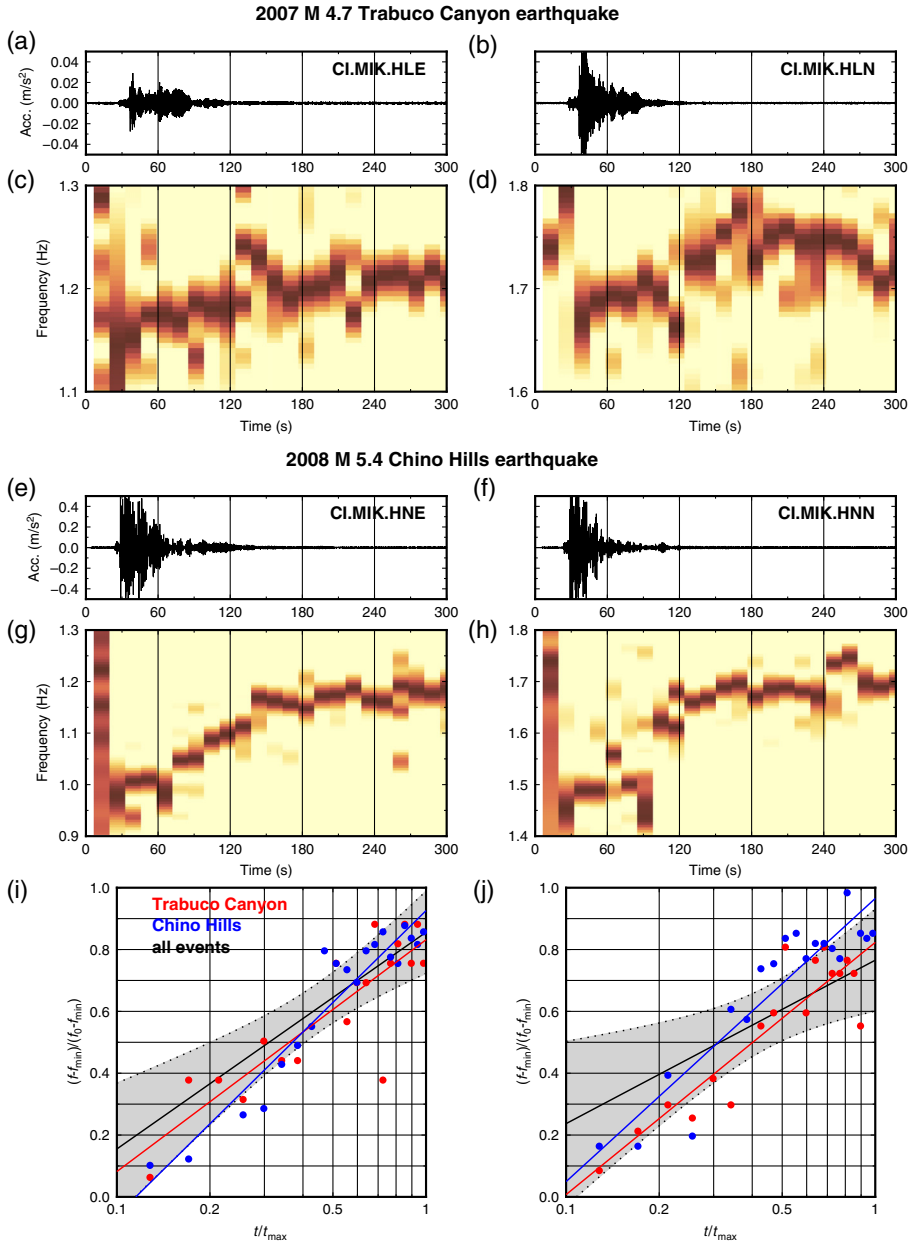

Figure 4. Nonlinear response and log–linear recovery for earthquakes with similar shaking duration but an order of magnitude difference in peak acceleration. (a,b) Acceleration recorded at CI.MIK in the east–west and north–south directions from the 2 September 2007 M 4.7 Trabuco Canyon earthquake (75 km epicentral distance). (c,d) Spectrograms of panels (a,b) showing near-instantaneous decrease in apparent fundamental frequencies at the onset of strong motion, followed by log–linear recovery over the scale of minutes. (e–h) Same as panels (a–d), but for the 29 July 2008 M 5.4 Chino Hills earthquake (39 km epicentral distance). (i) Peak frequencies in the east–west direction in each spectrogram time window (12.8 s) plotted as the fractional increase from the observed minimum frequency relative to the total coseismic drop, in which f_0 is the median frequency measured over an hour before each event. The scaled time has t = 0 30 s before the *S*-wave arrival and t_{max} = 300 s. (j) Same as panel (i) but for the north–south component. The red points and red linear regression represent the Trabuco Canyon earthquake from panels (c,d), the blue points and blue linear regression represent the Chino Hills earthquake from panels (g,h), and black represents the average across 54 earthquakes, the subset of all events in Figure 3 with peak acceleration >0.01 m/s^2 and excluding most aftershocks. Black dashed lines and shading represent one standard deviation of fitted slopes for all events.

time-invariant elasticity is an exceedingly poor assumption in the analysis of concrete structures.

Data and Resources

The seismographic data used in this study are available for public download through the Southern California Earthquake Data Center (SCEDC, 2013). Rainfall data from the Climate Hazards Group InfraRed Precipitation with Station data (CHIRPS) rainfall database (Funk *et al.*, 2014) is available at https://chc.ucsb.edu/data/chirps. Temperature data from the Global Historical Climatology Network daily (GHCNd) database (Menne *et al.*, 2012) is available at https://www.ncei.noaa.gov/data/global-historical-climatology-network-daily/. Soil moisture data from the Global Land Data Assimilation System (GLDAS-2.1) model (Rodell *et al.*, 2004) is available at https://disc.gsfc.nasa.gov/datasets/GLDAS_NOAH025_3H_2.1/summary. The supplemental material includes additional details of modal identification and forced vibration tests. All websites were last accessed in August 2022.

Declaration of Competing Interests

The authors acknowledge that there are no conflicts of interest recorded.

Acknowledgments

The authors thank Bob Nigbor, Steve Keowen, and Aileen

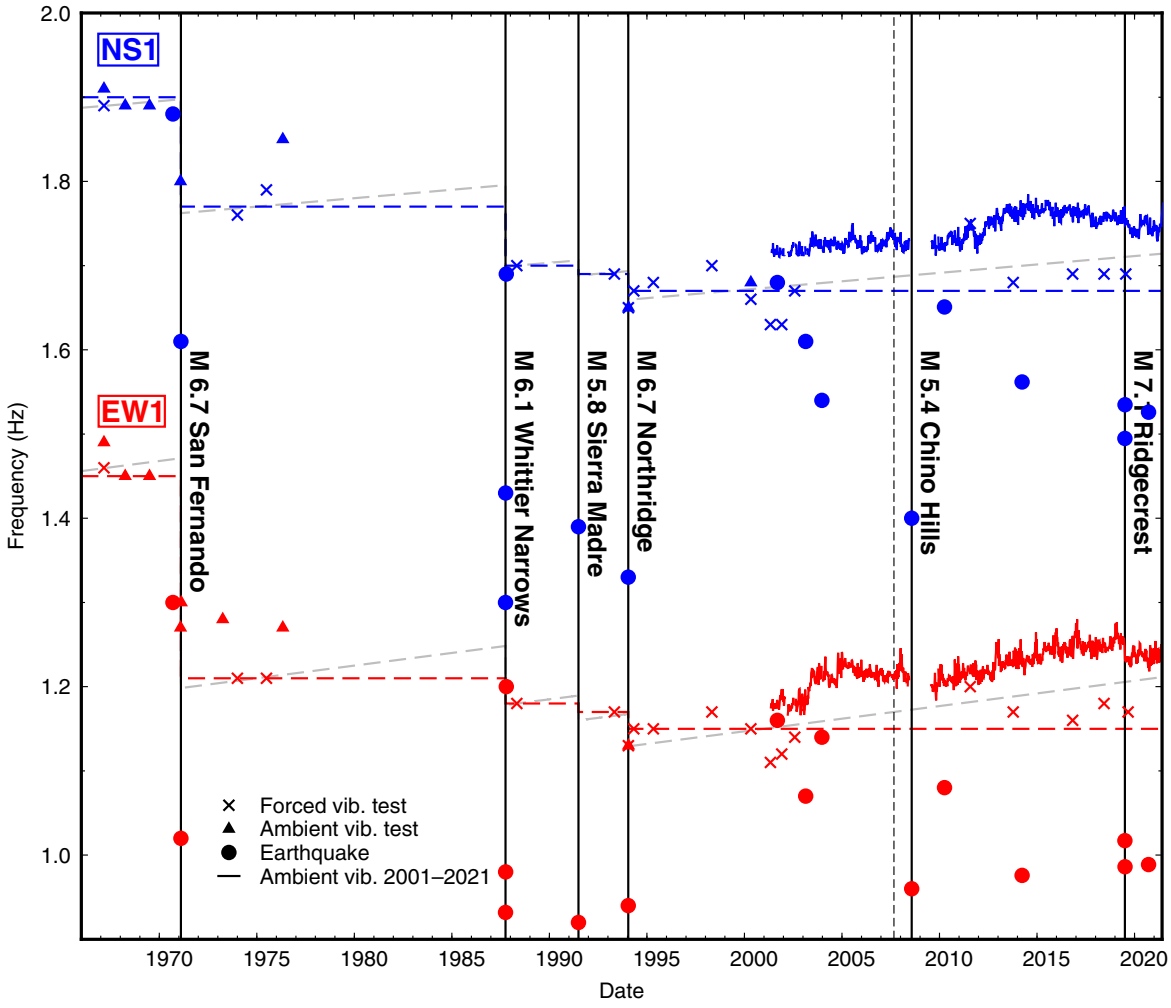

Zhang for their efforts refurbishing the Caltech Hall shaker in summer 2019, and Monica Kohler for insightful discussions that greatly improved this article. Ethan F. Williams was supported by a National Science Foundation (NSF) graduate research fellowship.

References

Astorga, A., and P. Gueguen (2020). Structural health building response induced by earthquakes: Material softening and recovery, *Eng. Rep.* **2,** e12228, doi: 10.1002/eng2.12228.

Astorga, A., P. Gueguen, and T. Kashima (2018). Nonlinear elasticity observed in buildings during a long sequence of earthquakes, *Bull. Seismol. Soc. Am.* **108,** no. 3A, 1185–1198.

Baker, J. W., B. A. Bradley, and P. J. Stafford (2021). *Seismic Hazard and Risk Analysis*, Cambridge University Press, Cambridge, United Kingdom, 581 pp.

Bradford, S. C., J. F. Clinton, J. Favela, and T. H. Heaton (2004). Results of Millikan Library forced vibration testing, *Earthquake Engineering Research Laboratory 2004-03*.

Figure 5. Lifetime changes in the east–west (red) and north–south (blue) fundamental frequencies of Caltech Hall, including ambient vibrations (triangles before 2001, solid lines after 2001), forced vibration tests (crosses), and major earthquakes (circles). Data are compiled from this study and Bradford *et al.* (2004). From left to right, the unlabeled significant earthquakes are 1970 **M** 5.2 Lytle Creek, 2001 **M** 4.2 Beverly Hills, 2003 **M** 5.4 Big Bear, 2003 **M** 6.6 San Simeon, 2010 **M** 7.2 El Mayor–Cucapah, 2014 **M** 5.1 Brea, and 2020 **M** 4.5 South El Monte. The 2007 **M** 4.7 Trabuco Canyon earthquake from Figure 4 is marked with a black dashed line. Colored dashed lines indicate the constant frequency between historical earthquakes speculatively inferred by Clinton *et al.* (2006) from forced vibration tests. Gray dashed lines schematically indicate the change in frequency that might have occurred between historical earthquakes if the long-term healing trend persisted before continuous instrumentation. Figure expanded from figure 2 of Clinton *et al.* (2006).

Clinton, J. F., S. C. Bradford, T. H. Heaton, and J. Favela (2006). The observed wander of the natural frequencies in a structure, *Bull. Seismol. Soc. Am.* **96,** no. 1, 237–257.

Edvardsen, C. (1999). Water permeability and autogenous healing of cracks in concrete, *ACI Mater. J.* **96,** 448–454.

Favela, J. (2004). Energy radiation from a multi-story building, *Ph.D. Thesis*, California Institute of Technology, Pasadena, California.

Foutch, D. A., and P. C. Jennings (1978). Foundation response of a nine-story reinforced concrete building, *Bull. Seismol. Soc. Am.* **68,** no. 1, 219–229.

Funk, C. C., P. J. Peterson, M. F. Landsfeld, D. H. Pedreros, J. P. Verdin, J. D. Rowland, B. E. Romero, G. J. Husak, J. C. Michaelsen, and A. P. Verdin (2014). A quasi-global precipitation time series for drought monitoring, *U.S. Geol. Surv. Data Series 832*, 4 pp.

Ghahari, S. F., F. Abazarsa, O. Avci, M. Celebi, and E. Taciroglu (2015). Blind identification of Millikan Library from earthquake data considering soil-structure interaction, *Struct. Control Health Monit.* **23,** 684–706.

Gueguen, P., P. Johnson, and P. Roux (2016). Nonlinear dynamics induced in a structure by seismic and environmental loading, *J. Acoust. Soc. Am.* **140,** 582–590.

Haselton, C. B., A. Fry, R. O. Hamburger, J. W. Baker, R. B. Zimmerman, N. Luco, K. J. Elwood, J. D. Hooper, F. A. Charney, R. G. Pekelnicky, *et al.* (2017). Response history analysis for the design of new buildings in the NEHRP provisions and ASCE/SEI 7 standard: Part II—Structural analysis procedures and acceptance criteria, *Earthq. Spectra* **33,** no. 2, 397–417.

Johnson, P., and A. Sutin (2005). Slow dynamics and anomalous nonlinear fast dynamics in diverse solids, *J. Acoust. Soc. Am.* **117,** no. 1, 124–130.

Kohler, M. D., P. M. Davis, and E. Safak (2005). Earthquake and ambient vibration monitoring of the steel-frame UCLA factor building, *Earthq. Spectra* **21,** no. 3, 1–22.

Kuriowa, J. H. (1967). Vibration test of a multistory building, *Ph.D. Thesis*, California Institute of Technology, Earthquake Engineering Research Laboratory, Pasadena, California.

Lees, T. P. (1992). Deterioration mechanisms, in *Durability of Concrete Structures: Investigation, Repair, Protection*, G. C. Mays (Editor), E. & F. N. Spon Press, London, United Kingdom, 10–36.

Luco, J. E., M. D. Trifunac, and H. L. Wong (1987). On the apparent change in dynamic behavior of a nine-story reinforced concrete building, *Bull. Seismol. Soc. Am.* **77,** no. 6, 1961–1983.

Luco, J. E., M. D. Trifunac, and H. L. Wong (1988). Isolation of soil-structure interaction effects by full-scale forced vibration tests, *Earthq. Eng. Struct. Dynam.* **16,** 1–21.

Menne, M. J., I. Durre, R. S. Vose, B. E. Gleason, and T. G. Houston (2012). An overview of the global historical climatology network-daily database, *J. Atmos. Ocean. Technol.* **29,** 897–910.

Moussa, M., A. P. Vassilopoulos, J. de Castro, and T. Keller (2013). Long-term development of thermophysical and mechanical properties of cold-curing structural adhesives due to post-curing, *J. Appl. Polym. Sci.* **127,** no. 4, 2490–2496.

Rodell, M., P. R. Houser, U. Jambor, J. Gottschalck, K. Mitchell, C.-J. Meng, K. Arsenault, B. Cosgrove, J. Radakovich, M. Bosilovich, *et al.* (2004). The global land data assimilation system, *Bull. Am. Meteor. Soc.* **85,** no. 3, 381-394.

Roig-Flores, M., and P. Serna (2020). Concrete early-age crack closing by autogenous healing, *Sustainability* **12,** 4476.

SCEDC (2013). Southern California Earthquake Data Center, *Caltech Dataset*, doi: 10.7909/C3WD3xH1.

TenCate, J. A., E. Smith, and R. A. Guyer (2000). Universal slow dynamics in granular solids, *Phys. Rev. Lett.* **85,** no. 5, 1020–1023.

Todorovska, M. I. (2009a). Soil-structure system identification of Millikan Library north-south response during four earthquakes (1970-2002): What caused the observed wandering of the system frequencies? *Bull. Seismol. Soc. Am.* **99,** no. 2A, 626–635.

Todorovska, M. I. (2009b). Seismic interferometry of a soil-structure interaction model with coupled horizontal and rocking response, *Bull. Seismol. Soc. Am.* **99,** no. 2A, 611–625.

Todorovska, M. I., and Y. Al Rjoub (2006). Effects of rainfall on soil-structure system frequency: Examples based on poroelasticity and a comparison with full-scale measurements, *Soil Dynam. Earthq. Eng.* **26,** nos. 6/7, 708–717.

Trifunac, M. D., S. S. Ivanovic, and M. I. Todorovska (2001). Apparent periods of a building, II: Time-frequency analysis, *J. Struct. Eng.* **127,** no. 5, 527–537.

Udwadia, F. E., and M. D. Trifunac (1974). Time and amplitude dependent response of structures, *Earthq. Eng. Struct. Dynam.* **2,** 359–378.

Zimmerman, R. B., J. W. Baker, J. D. Hooper, S. Bono, C. B. Haselton, A. Engel, R. O. Hamburger, A. Celikbas, and A. Jalalian (2017). Response history analysis for the design of new buildings in the NEHRP provisions and ASCE/SEI 7 standard: Part III—Example applications illustrating the recommended methodology, *Earthq. Spectra* **33,** no. 2, 419–447.

Manuscript received 12 August 2022
Published online 8 November 2022